ADMET & DMPK **14** (2026) 3618*; doi: https://doi.org/10.5599/admet.3618*

ADMET

Open Access : ISSN : 1848-7718

http://www.pub.iapchem.org/ojs/index.php/admet

Original scientific paper

Cu-metal-organic framework/multi-walled carbon nanotubes modified glassy carbon electrode for voltammetric determination of anticancer drug calcium folinate

Hassan Ali M. Jawad

College of Pharmacy, Alfarahdi University, Baghdad, Iraq

Corresponding Author: E-mail: *hassanalimohammed@uoalfarahidi.edu.iq*

Received: August 9, 2026; Revised: October 11, 2026; Published: Octobar 26, 2026

Abstract

Background and purpose: Maintaining therapeutic efficacy, avoiding toxicity, and ensuring appropriate dosing all depend on accurate calcium folinate (CLF) measurement. Additionally, it is essential for therapeutic drug monitoring, especially for patients undergoing high-dose methotrexate therapy. **Experimental approach:** We modified the surface of a glassy carbon electrode (GCE) to detect CLF using a Cu-based metal-organic framework integrated with multi-walled carbon nanotubes (Cu-MOF/CNTs). The combined action of CNTs and Cu-MOF significantly enhanced the performance of the GCE surface. **Key results**: When CLF was quantified by differential pulse voltammetry, the Cu-MOF/CNTs/GCE showed a strong linear response across 0.08 to 450.0 µM. Additionally, the sensing platform demonstrated sensitivity of 0.0879 µA μM^{-1} toward CLF and a low limit of detection of 0.02 µM. **Conclusion:** CLF in actual samples was successfully determined using Cu-MOF/CNTs-modified GCE, showing acceptable efficiency.

©2026 by the authors. This article is an open-access article distributed under the terms and conditions of the Creative Commons Attribution license (http://creativecommons.org/licenses/by/4.0/).

Keywords

Folinic acid; modified electrode; real sample analysis; drug analysis

Introduction

Calcium folinate (CLF), or leucovorin calcium, is biologically active and can immediately support folate-dependent metabolic activities, unlike folic acid, which must be activated via dihydrofolate reductase. By bypassing this enzymatic step, it restores decreased intracellular folate levels, which are necessary for the synthesis of purines, thymidylate, and many amino acids. Because of these pharmacological characteristics, CLF is important in toxicology, cancer, and supportive care. Rescue therapy after high-dose methotrexate treatment is one of CLF's main clinical uses [1].

Methotrexate depletes folate levels and disrupts DNA synthesis in both malignant and quickly dividing normal cells by inhibiting dihydrofolate reductase. When patients adhere to the prescribed treatment plan, timely administration of CLF refills intracellular folate pools in healthy tissues, reducing methotrexate's toxic effects without significantly affecting its anticancer effectiveness [2]. Combining CLF with 5-fluorouracil is another significant therapeutic application. In this context, it stabilizes the ternary complex formed between decreased folates, thymidylate synthase and fluorodeoxyuridine monophosphate, increasing the anticancer activity of fluorouracil [3]. This complex's enhanced stability sustains DNA synthesis and thymidylate production suppression, prolonging thymidylate synthase inhibition [3].

As a result, fluorouracil's cytotoxic effects on tumour cells are amplified, increasing chemotherapy's overall efficacy [3]. Although CLF is usually well tolerated, improper dosing can reduce the therapeutic effectiveness of antifolate medicines. Additionally, it can lower the plasma concentrations of some antiepileptic medications, such as primidone, phenytoin, and phenobarbital, which may raise the risk of seizure recurrence in individuals who are vulnerable. Therefore, when CLF is used with these drugs, close clinical observation is advised. Capillary electrophoresis (CE) [4], high-performance liquid chromatography (HPLC) [5], fluorescence [6], and electrochemistry [7] have all been used to study CLF.

While these approaches are effective, they usually involve complicated procedures. Among these approaches, straightforward, fast, sensitive, and affordable electrochemical techniques have gained popularity. These techniques allow direct compound identification, require little preparation, and avoid time-consuming pretreatment, reducing analysis time and cost [8].

Furthermore, electrochemical methods provide vital information about the pharmacological activities of medicinal molecules and make it easier to identify their redox characteristics [9]. However, high redox potentials and the limited sensitivity of electroactive compounds on unaltered electrode surfaces make trace-level measurement difficult. Electrode surface modification can address or mitigate these issues. Surface modification also improves electrode kinetics, increasing detection sensitivity and selectivity. Creating highly sensitive electrochemical sensors for medical diagnostics has proven difficult and remains in high demand in recent years [10].

Deliberate chemical modification of electrode with modifiers can efficiently control the speed and selectivity of electrochemical processes [10]. Glassy carbon electrodes (GCE) have shown notable stability and resistance among the various electrode types used in electrochemical measurements. Because electron transfer is sluggish at ordinary electrodes, redox reactions in electroanalytical procedures often require a large overpotential. Furthermore, interest in modifying conventional electrodes is increasing because they often perform poorly in analyte detection. According to earlier research, electrode surface modification increases electron-transport rate while also considerably lowering overpotentials [11,12].

By manipulating matter at the nanoscale, nanotechnology is a new, fundamental technology that enables the creation of unique materials and tools. The extraordinary potential of nanoparticles in a variety of applications has been the focus of extensive research over the last few decades. Their unique physicochemical characteristics have been the subject of numerous investigations, making them especially useful for a variety of application domains [9].

In particular, nanomaterials in electrochemical sensors have enabled the development of effective instruments for food safety, medical diagnostics, and environmental monitoring [9]. Metal ions and organic linkers are the two primary constituents of MOFs, a class of materials with highly porous structures. These materials have high porosity, configurable pore size and structure, vast surface areas, diverse dimensions and morphologies, programmable surface properties, and abundant adsorption sites [13].

These features make MOFs a groundbreaking development in materials science because they offer potent and efficient solutions to problems in medicine, energy, the environment, gas storage and separation, sensors, *etc*. [13]. Electrochemical sensing is a well-known application of MOFs. However, because MOFs are poorly conductive, problems with their direct application in electrocatalysis still exist. Using other materials in MOF preparation can address these problems. Carbon materials seem to be the most appropriate choice in this case owing to their conductivity and electrochemical stability. One of the most suitable candidates for MOF composite creation is carbon nanostructures (*e.g.* CNTs) [14]. CNTs are formed by the complex arrangement of carbon modules into several cylinders of graphite. The homogenous distribution of the

(cc) BY

electron clouds of carbon enables the high conductivity of MWCNTs because the electron clouds spread from carbon atoms to tubular shapes. In fact, materials containing MWCNTs are often used to transport electrons from electrodes to analysers because of the material's superb conductivity and high specific surface area. Using MWCNTs can increase a material's conductivity. Because of these benefits, integrating MWCNTs with MOFs to improve their electrochemical performance is very appealing [15]. MOF- and MWCNT-based nanocomposites are expected to show synergistic effects that enhance electrochemical sensing efficiency while retaining the benefits of each component [16].

In this work, we present a suitable voltammetric technique for determining CLF using Cu-MOF/CNTs/GCE. Because Cu-MOF and CNTs work well together, Cu-MOF/CNTs/GCE performs well when it comes to CLF determination. Additionally, the Cu-MOF/CNTs/GCE sensing device, as constructed, demonstrated a high sensitivity for CLF determination. Additionally, the sensing platform was used to measure CLF in actual samples to assess its usefulness.

Experimental

Electrochemical experiments

Cyclic voltammetry (CV) studies were done to investigate the behaviour of CLF. The first examined the effect of scan rate on the response and was done by extracting CVs at different scan rates. The working electrode was then held at a fixed step potential of 550 mV for 15 s to perform chronoamperometric determination of the diffusion coefficient of CLF. Differential pulse voltammetry (DPV) in PBS at various concentrations with CLF was utilized for quantitative determinations.

Materials and instrumentations

All electrochemical experiments were conducted using a potentiostat/galvanostat AUTOLAB PGSTAT 12N (Metrohm, Herisau, Switzerland) and monitored using the General-Purpose Electrochemical System (GPES) software. The solution's pH was measured using 713 pH meter (Metrohm, Herisau, Switzerland) fitted with a glass electrode. All solutions were prepared using deionized water from the Direct-Q 8UV water purification system (Millipore, Darmstadt, Germany).

All chemicals and reagents were analytical grade (Merck and US Nanotech). They were used in this work as supplied, requiring no additional purification. Phosphoric acid (0.1 M) was used to generate phosphate buffer solution (PBS), which serves as the supporting electrolyte solution at a specific pH. The pH was adjusted using an aqueous NaOH solution.

Synthesis of Cu-based metal-organic framework integrated with multi-walled carbon nanotubes

With a few minor adjustments, such as the incorporation of COOH-functionalized multi-walled carbon nanotubes (COOH-f-MWCNTs), the synthesis of Cu-MOF/COOH-f-MWCNTs was carried out using the method outlined by Sakthivel *et al.* [17]. To create a homogenous solution, $Cu(NO_3)_2{\cdot}3H_2O$ (1 mmol) was dissolved in 12 mL of methanol, 0.62 mL of acetic acid and 0.42 mL of triethylamine while being magnetically stirred for 60 minutes. Next, benzene-1,3,5-tricarboxylic acid (BTC) (1 mmol) was dissolved in the aforementioned solution. The as-prepared precursors were then combined with 0.004 g of COOH-f-MWCNTs and ultrasonicated for 60 minutes at room temperature. Next, the suspension was placed in an autoclave for 24 hours at 85 °C. After cooling, the mixture was centrifuged, and the recovered product underwent five consecutive ethanol washes. Lastly, the cleaned product was dried overnight at 67 °C in an oven. In contrast, the same process was used to create Cu-MOF without COOH-f-MWCNTs.

Preparation of the modified glassy carbon electrode

To prepare Cu-MOF/CNTs/GCE, the GCE was first polished with alumina slurry. Next, 0.5 mg of Cu-MOF/CNTs was dispersed in 0.5 mL of water. Finally, 4.0 µL of the suspension was drop-cast onto the GCE surface.

Preparation of calcium folinate injection and urine samples

First, a 100 mL volumetric flask was filled with CLF injection and diluted using PBS. To quantify these species, the unspiked injection sample and the spiked injection sample containing standard solutions of CLF were moved to the electrochemical cell and concentrations were determined by DPV.

A 0.45 µm filter was used to filter 10 mL of the urine sample after centrifugation for 10 minutes at 3000 rpm. Next, different quantities of CLF were added to a 25 mL volumetric flask containing 5 mL of filtrate, which was then diluted with PBS (pH 7). This solution was used for the measurements in the next step.

Results and discussion

Comparing the voltammetric behaviour of calcium folinate on the unmodified glassy carbon electrode surface and Cu-based metal-organic framework integrated with multi-walled carbon nanotubes glassy carbon electrode surface

The differential pulse voltammetry responses of CLF were recorded at the Cu-MOF/CNTs/GCE, with a pH value range of 4.0 to 9.0, to assess the impact of pH on the CLF voltammetric response (Figure 1). According to DPV measurements, the peak current (*I*) for CLF determination initially rises as pH increases from 4.0 to 7.0, with neutral conditions yielding the maximum *I*. As pH increases from 7.0 to 9.0, the current progressively decreases. Therefore, the ideal pH for determining CLF at the Cu-MOF/CNTs/GCE is 7.0 in 0.1 M PBS (Figure 2A).

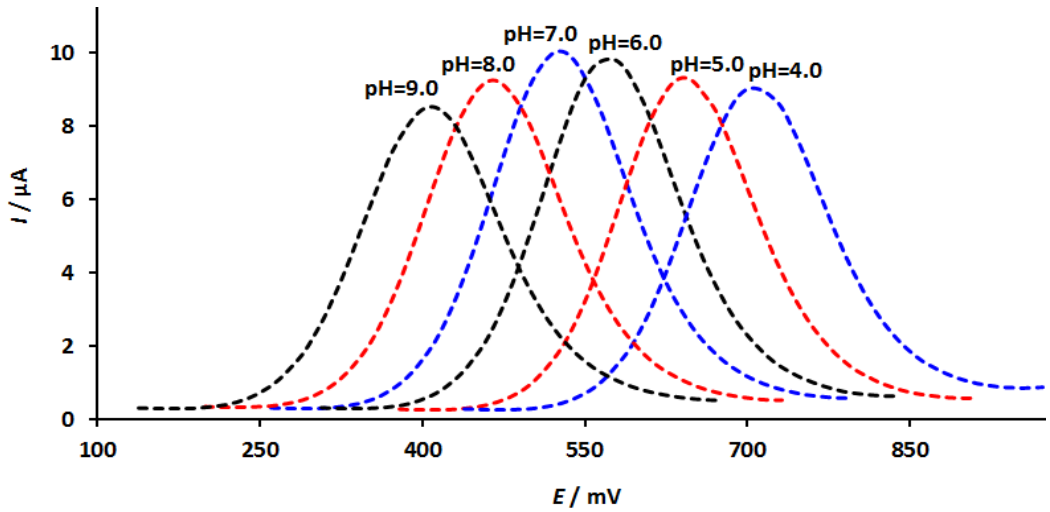


Figure 1. DPV responses of Cu-MOF/CNTs/GCE in PBS containing 100.0 µM CLF prepared at different pH (4.0 to 9.0).

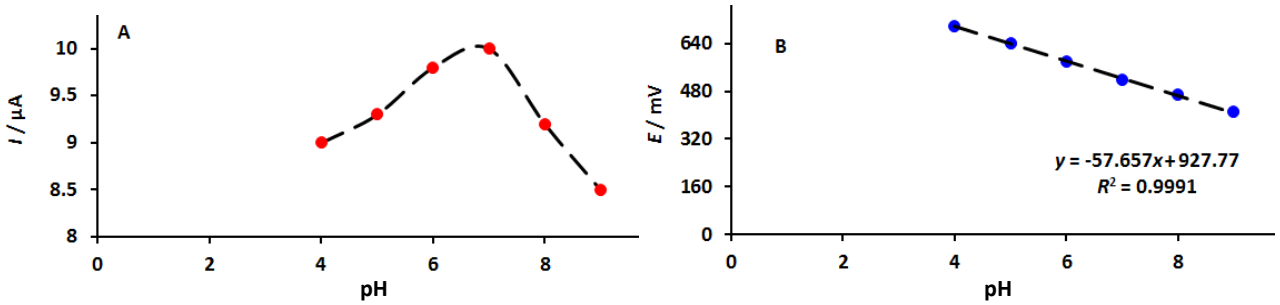


Figure 2. Dependence of *I* on pH (A) and dependence of *E* on pH (B) for CLF at the Cu-MOF/CNTs/GCE

(cc) BY

Furthermore, as pH increased, the anodic peak potentials of CLF shifted to less positive values. As shown in Figure 2B, the equation was E = -57.657 pH + 927.77 (R^2 = 0.9991). Peak potential (E) and pH showed a linear relationship, with a slope of -57.657 mV pH^{-1} for CLF. This slope suggests that CLF oxidation involves the transfer of two electrons and two protons. These findings demonstrate how crucial *p*H is to maximizing the Cu-MOF/CNTs/GCE sensor's performance for CLF detection.

The cyclic voltammograms (CVs) of 100.0 µM CLF on unmodified GCE (a) and Cu-MOF/CNTs/GCE (b) are shown in Figure 3. The current (I) of CLF at Cu-MOF/CNTs/GCE and unmodified GCE was 9.86 and 4.00 µA, respectively. It is evident that the I of CLF increased in comparison to the unmodified GCE. Additionally, compared with the unmodified GCE (voltammogram a), the anodic peak potential shifted toward more negative values, suggesting that the modified electrode catalytically promoted CLF oxidation.

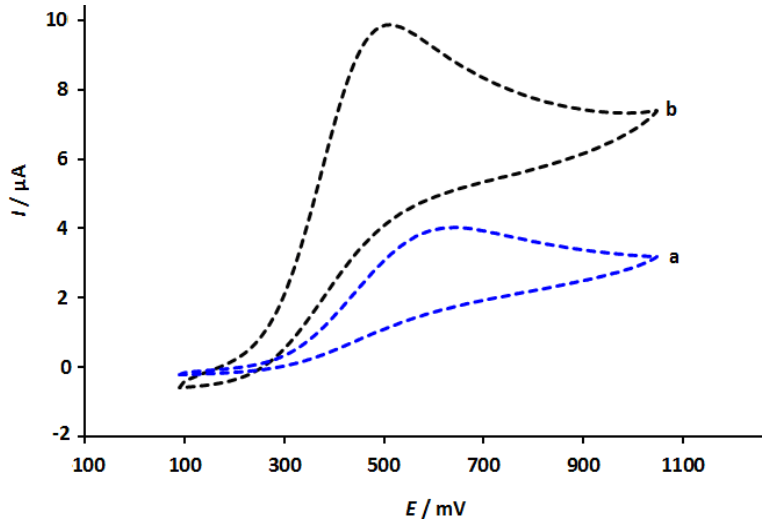


Figure 3. CV curves of 100.0 µM CLF by bare GCE (a) and Cu-MOF/CNTs/GCE at 50 mV s^{-1}

Effect of scan rate on electrochemical behaviour of calcium folinate

Increasing the scan rate may amplify the peak oxidation currents, as shown by the results of assessing the impact of scan rate on the CLF oxidation current (Figure 4). I and $v^{1/2}$ showed a linear relationship, indicating a diffusion-controlled oxidation process.

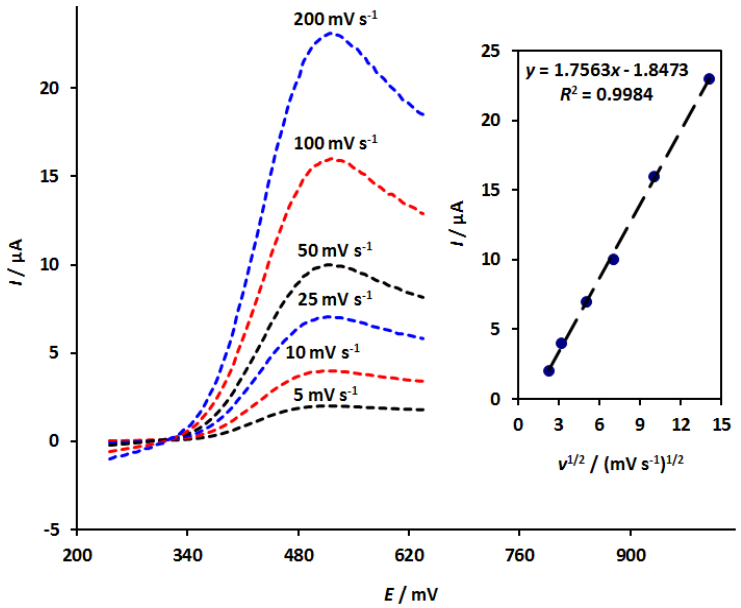


Figure 4. Linear scan voltammetry curves of 100.0 µM CLF by Cu-MOF/CNTs/GCE at various scan rates. Inset: the relationship between I and the $v^{-1/2}$

Chronoamperometric investigations

Chronoamperograms for CLF in PBS at Cu-MOF/CNTs/GCE are presented in Figure 5. The chronoamperogram clearly shows the dependence of current on time for CLF at different concentrations. First, the current decays sharply and then slowly stabilize as time passes, indicating that the electrochemical reaction is diffusion-controlled. Figure 6A shows the linear relationship between current and $t^{-1/2}$, calculated from the chronoamperograms. These kinds of plots are referred to as Cottrell plots. Next, the slopes in Figure 6A were plotted against the CLF concentrations (Figure 6B). Finally, by employing the slope in Figure 6B and Cottrell's equation ($I = nFACD^{1/2}/(\pi t)^{1/2}$), the diffusion coefficient of CLF at Cu-MOF/CNTs/GCE was calculated as 2.6×10^{-5} cm^2 s^{-1}.

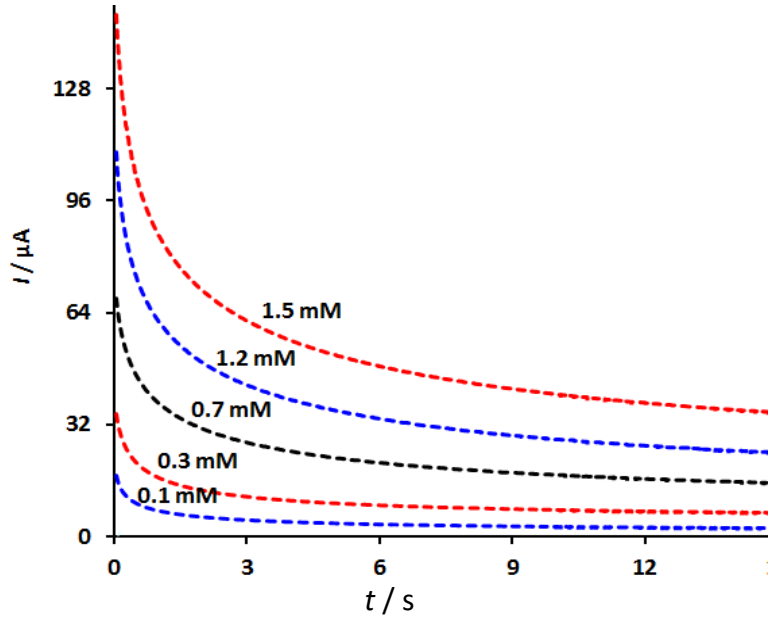


Figure 5. Chronoamperograms at Cu-MOF/CNTs/GCE for different concentrations of CLF

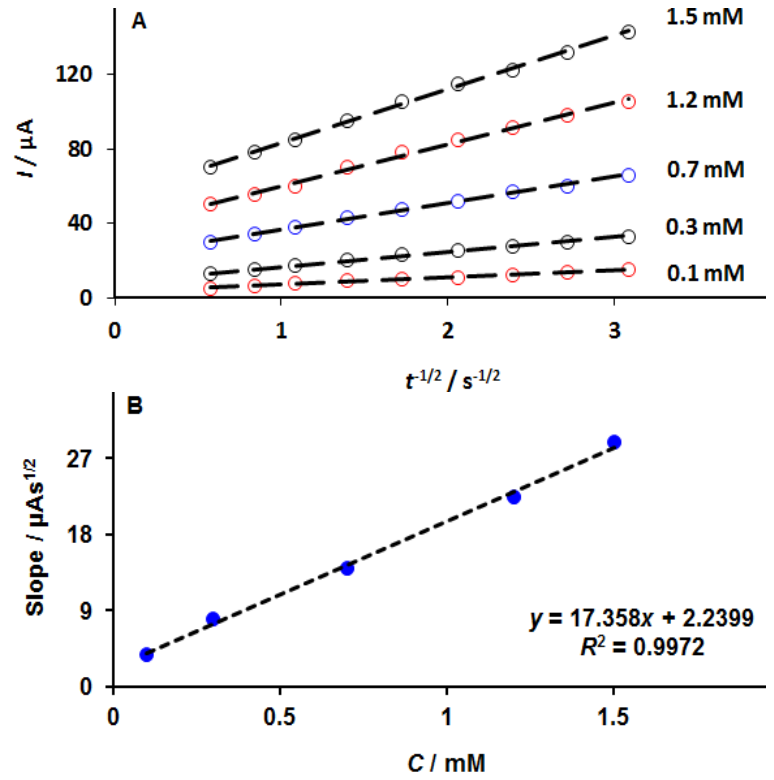


Figure 6. (A) Plots of *I vs.* $t^{-1/2}$; (B) Plot of the slope against CLF concentration

CC BY

Calibration curve

Cu-MOF/CNTs/GCE treated to specific CLF concentrations showed DPVs between 0.083 and 450.0 µM (Figure 7). $I = 0.0879C + 1.2467$ ($R^2 = 0.9995$) is the fitting equation that was obtained (Figure 7, inset). Lastly, the limit of detection (LOD) of the intended sensing platform can be determined using Equation (1):

$$LOD = 3S_{Blank}/m \quad (1)$$

In this case, m is the slope value obtained from the calibration plot, and S_{Blank} is the standard deviation of 12 blank data points without CLF. LOD was determined to be 0.02 µM.

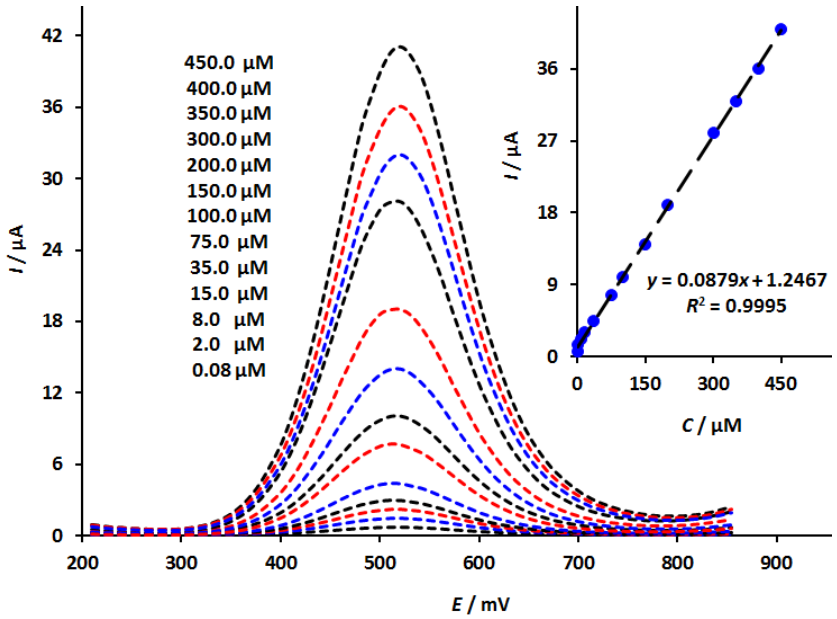


Figure 7. DPVs accepted Cu-MOF/CNTs/GCE in diverse concentrations of CLF. Inset: plot of *I* versus CLF concentration

Repeatability, stability and reproducibility

Because repeatability, stability and reproducibility directly affect the accuracy and dependability of an electrochemical sensor, assessing them is essential to evaluating sensor performance. To assess long-term stability, the current response to CLF (50.0 µM) over four weeks was tracked. The response peak current decreased slightly. After four weeks, the reaction peak current to CLF remained at 95.5 % of its starting value. Additionally, 10 consecutive DPV measurements of 50.0 µM CLF were used to evaluate the Cu-MOF/CNTs/GCE sensor's repeatability. With a relative standard deviation (RSD) of 3.9 %, the DPV readings offered good repeatability. Additionally, 8 identical sensors were used to detect 50.0 µM CLF by DPV to evaluate the repeatability of the Cu-MOF/CNTs/GCE sensor. The maximum current response RSD was 3.7 %. These results support the outstanding repeatability, reproducibility and storage stability of Cu-MOF/CNTs/GCE.

Interference studies

Different species in real samples can affect an electrode's ability to detect and respond sensitively. We examined the variations in current of CLF to investigate the interference effects of these species. As a result, one important aspect influencing monitoring accuracy is the modified electrode's anti-interference capability. This investigation shows that the sensitivity of Cu-MOF/CNTs/GCE is not greatly affected by other interferences, even at concentrations several times higher than those of CLF.

For example, in the detection of CLF using Cu-MOF/CNTs/GCE, a 200-fold concentration of Mg^{2+}, NH^{4+}, Ca^{2+}, and Fe^{3+} resulted in slight changes in the peak current (less than 5 %). Similarly, a 10-fold concentration of dopamine, tartaric acid, vitamin C, glucose, tryptophan, L-cysteine, and sucrose caused signal changes of less

than 5 % when using the same electrode for CLF detection. The measurement conditions were the same. These species had no discernible impact on the developed sensor's voltammetric response for CLF determination.

Analytical application

Lastly, CLF analysis of the CLF injection and urine samples, along with recovery measures, evaluated implementation of the recommended method. The actual sample's CLF content was first ascertained. The actual samples were then spiked with different CLF concentrations. Table 1 displayed the analysis's findings. The spiked samples had recovery values ranging from 97.1 to 103.7 %. Likewise, the RDSs (n = 5) were below 3.6 %. Therefore, the recommended sensing platform might be used to determine CLF in pharmaceutical samples with good outcomes.

Table 1. Voltammetric determination of CLF in real specimens at Cu-MOF/CNTs/GCE (n=5)

Sample	Amount, µM		Recovery, %	RSD, %
	Added	Found		
CLF injection	0	3.9	-	2.8
	1.0	5.0	102.0	3.0
	3.0	6.7	97.1	2.2
	5.0	8.8	98.9	2.7
	7.0	11.3	103.7	1.9
Urine	5.0	4.9	98.0	1.8
	7.0	7.2	102.9	3.6
	9.0	8.8	97.8	2.3
	11.0	11.4	103.6	2.5

Conclusion

In this work, a low-cost, easy-to-fabricate Cu-MOF/CNTs/GCE sensor was developed to detect CLF in real samples. The CPE-modified sensor showed a low LOD of 0.002 µM and a broad LDR for CLF from 0.05 to 450.0 µM. Practical applicability of the electrochemical sensor was verified by analysing actual samples (CLF ampule and urine), which produced recovery rates ranging from 97.1 to 103.7 % and an RSD of less than 3.6 %.

References

[1] N. Tubiana-Mathieu, S. Monjanel-Mouterde, C. Lejeune, B. Payet, J. Catalin, Y. Carcassonne, J. Cano. Pharmacokinetics of folinic acid and 5-methyltetrahydrofolic metabolite after repeated oral administration of calcium folinate following methotrexate treatment. *European Journal of Cancer* **30** (1994) 1281-1284. https://doi.org/10.1016/0959-8049(94)90173-2

[2] X. J. Yang, Y. P. Chen, H. C. Wang, J. Zhao, F. Y. Zheng. Protective effect of calcium folinate against methotrexate-induced endosalpinx damage in rats. *Fertility and Sterility* **95** (2011) 1526-1530. https://doi.org/10.1016/j.fertnstert.2010.08.028

[3] E. Topuz, M. Basaran, P. Saip, A. Aydiner, A. Argon, B. Sakar, F. Tas, K. Uygun, D. Bugra, N.F. Aykan. Adjuvant intraperitoneal chemotherapy with cisplatinum, mitoxantrone, 5-fluorouracil, and calcium folinate in patients with gastric cancer: a phase II study. *American Journal of Clinical Oncology* **25** (2002) 619-624. https://doi.org/10.1016/S0959-8049(99)80983-6

[4] J. Yu, X. Liang, Z. Wang, X. Guo, T. Sun, X. Guo. Separation of folinic acid diastereomers in capillary electrophoresis using a new cationic β-cyclodextrin derivative. *Plos One* **10** (2015) e0120216. https://doi.org/10.1371/journal.pone.0120216

[5] G. Francese, F. Corana, O. Meneghetti, F. Marazza. LC–MS characterization of trace impurities contained in calcium folinate. *Journal of Pharmaceutical and Biomedical Analysis* **39** (2005) 757-763. https://doi.org/10.1016/j.jpba.2005.04.014

(cc) BY

[6] I. D. Merás, A. Espinosa-Mansilla, M.J. Gómez, F. S. López. Kinetic fluorimetric study of the oxidation reaction of folinic acid (leucovorin) with potassium permanganate. Determination in human urine. *Talanta* **55** (2001) 623-630. https://doi.org/10.1016/S0039-9140(01)00472-6

[7] Z. Zhu, F. Wang, F. Wang, L. Xi. Simultaneous determination of methotrexate and calcium folinate with electrochemical method based on a poly-ABSA/functionalized MWNTs composite film modified electrode. *Journal of Electroanalytical Chemistry* **708** (2013) 13-19. https://doi.org/10.1016/j.jelechem.2013.09.004

[8] O. A. Sadik, A. O. Aluoch, A. Zhou. Status of biomolecular recognition using electrochemical techniques. *Biosensors and Bioelectronics* **24** (2009) 2749-2765. https://doi.org/10.1016/j.bios.2008.10.003

[9] W. A. Yue-Rong, H. U. Ping, L. U. Guo-An, W. A. Yi-Ming. Application of carbon nanotube modified electrode in bioelectroanalysis. *Chinese Journal of Analytical Chemistry* **36** (2008) 1011-1016. https://doi.org/10.1016/S1872-2040(08)60052-3

[10] M. Opallo, A. Lesniewski. A review on electrodes modified with ionic liquids. *Journal of Electroanalytical Chemistry* **656** (2011) 2-16. https://doi.org/10.1016/j.jelechem.2011.01.008

[11] W. E. Van der Linden, J. W. Dieker, Glassy carbon as electrode material in electro-analytical chemistry. *Analytica Chimica Acta* **119** (1980) 1-24. https://doi.org/10.1016/S0003-2670(00)00025-8

[12] P. Lakhera, V. Chaudhary, A. Jha, R. Singh, P. Kush, P. Kumar. Recent developments and fabrication of the different electrochemical biosensors based on modified screen printed and glassy carbon electrodes for the early diagnosis of diverse breast cancer biomarkers. *Materials Today Chemistry* **26** (2022) 101129. https://doi.org/10.1016/j.mtchem.2022.101129

[13] Z. Zhang, Y. Lou, C. Guo, Q. Jia, Y. Song, J. Y. Tian, S. Zhang, M. Wang, L. He, M. Du. Metal–organic frameworks (MOFs) based chemosensors/biosensors for analysis of food contaminants. *Trends in Food Science & Technology* **118** (2021) 569-588. https://doi.org/10.1016/j.tifs.2021.10.024

[14] N. Ma, A. Wei, H. Peng, L. Xie, Y. Jin, Z. Yin, G. Li. A chiral electrochemical sensor based on β-CD/Ce-doped Cu-MOF/MWCNTs-COOH for enantioselective recognition and detection of levofloxacin. *Analytica Chimica Acta* **1420** (2026) 345964. https://doi.org/10.1016/j.aca.2026.345964

[15] L.X. Xia, T.T. Liu, S.T. Zhang, W.Y. Pei, J.F. Ma. Electrochemical determination of trace Cu (II) and Pb (II) with a new sensor constructed by a composite of cyclotriguaiacylene MOF/MWCNT-COOH. *Journal of Molecular Structure* **1378** (2026) 147217. https://doi.org/10.1016/j.molstruc.2026.147217

[16] G.M. Jaid, A.A. AbdulRazak, M. al-Shaeli, Q.F. Alsalhy, R.A. Al-Juboori.Plastic waste-based Cu-BDC and COOH-MWCNT@ Cu-BDC MOF for enhancing PPSU membrane for efficient heavy metal removal from industrial wastewater. *Journal of Environmental Chemical Engineering* **14** (2025) 120608. https://doi.org/10.1016/j.jece.2025.120608.

[17] R. Sakthivel, L.Y. Lin, Y.F. Duann, H.H. Chen, C. Su, X. Liu, J.H. He, R.J. Chung. MOF-derived Cu-BTC nanowire-embedded 2D leaf-like structured ZIF composite-based aptamer sensors for real-time in vivo insulin monitoring. *ACS Applied Materials & Interfaces* **14** (2022) 28639-28650. https://doi.org/10.1021/acsami.2c06785

©2026 by the authors; licensee IAPC, Zagreb, Croatia. This article is an open-access article distributed under the terms and conditions of the Creative Commons Attribution license (http://creativecommons.org/licenses/by/4.0/)